ORIGINAL ARTICLE

Predicting IDH mutation status of lower grade gliomas using standard MR imaging features and apparent diffusion coefficient

Shuangshuang Song[1,2] · Jiankun Xu[3] · Leiming Wang[4] · Fan Yu[1,2] · Yueshan Piao[4] · Miao Zhang[1,2] · Jie Lu[1,2]

Abstract

Purpose The purpose of this study was to investigate the predictive value of standard MR imaging features and apparent diffusion coefficient (ADC) values as specific markers for isocitrate dehydrogenase (IDH)-mutated lower grade gliomas (LGGs).

Materials and methods Standard MR imaging features including location, T2-FLAIR mismatch sign, signal heterogeneity, margin, growth pattern, degree of enhancement and peritumoral edema, and ADC parameters of 74 LGGs were retrospectively assessed. The values of these imaging features in predicting IDH genotypes were further analyzed.

Results Inter-rater agreement of T2-FLAIR mismatch sign reached the highest κ value. The specificity of T2-FLAIR mismatch sign to predict IDH-mutated LGGs was 100%. IDH-mutated LGGs also tended to manifest single-lobe invasion, distinct margin, less degree of contrast enhancement and peritumoral edema, and higher normalized minimum and mean ADC than IDH-wildtype LGGs (all $P < 0.05$). The sensitivity, specificity, and AUC of the combination of the imaging features and ADC parameters to predict IDH genotypes were 81.82%, 86.67%, and 0.925, respectively ($P < 0.001$).

Conclusion Standard MRI could clearly show the imaging features of different IDH subtypes of gliomas, which could be easily applied in clinical practice and helpful to use in predicting IDH mutation status of LGGs non-invasively.

Keywords Glioma · Magnetic Resonance Imaging (MRI) · Isocitrate dehydrogenase (IDH) · Diffusion magnetic resonance imaging

Introduction

Gliomas are one of the most common primary malignant tumors of the central nervous system with high mortality and disability rate [1]. World Health Organization (WHO) classification system incorporated molecular biomarkers into the classification of gliomas in 2016 including the important isocitrate dehydrogenase (IDH) mutation [2, 3]. It is a robust diagnostic and prognostic biomarker for lower grade gliomas (LGGs) including WHO grade II and III gliomas [4]. LGGs with similar histological characteristics may have diverse outcomes between individuals due to different IDH genetic backgrounds [5]. More than 75% of LGGs are IDH-mutated, which are more sensitive to chemotherapy, easy to completely resect, and with longer overall survival comparing to IDH-wildtype gliomas [6].

At present, tumor tissue sampling for genetic analysis is the most reliable method to detect IDH mutation status. However, it is invasive and may cause unnecessary damage to patients who only need follow-up or chemotherapy. As a result, failure to accurately diagnose IDH genotypes will affect the subsequent treatment. Therefore, exploring a noninvasive method to identify the status of IDH mutation of gliomas before treatment is of vital importance [7, 8].

Conventional and contrast-enhanced MRI and diffusion-weighted imaging (DWI) are standard clinical examinations for gliomas. They are feasible for a majority of hospitals. It would make sense if standard MR imaging features could non-invasively predict IDH genotypes of glioma before treatment. Patel et al. [9] indicated that

✉ Jie Lu
   imaginglu@hotmail.com

1   Department of Radiology and Nuclear Medicine, Xuanwu Hospital, Capital Medical University, No.45 Changchun Street, Xicheng District, Beijing, People's Republic of China

2   Beijing Key Laboratory of Magnetic Resonance Imaging and Brain Informatics, Beijing, China

3   Department of Radiation Oncology, Xuanwu Hospital, Capital Medical University, Beijing, China

4   Department of Pathology, Xuanwu Hospital, Capital Medical University, Beijing, China

T2-FLIAR mismatch sign may correlate with the status of IDH and 1p/19q co-deletion. It presented a homogeneous hyperintense signal on T2-weighted imaging (T2WI) and comparatively hypointense on fluid-attenuated inversion recovery images (FLAIR) with a hyperintense ring-shaped margin. However, not all of the IDH-mutated gliomas would present the T2-FLAIR mismatch sign. Tumor location, signal heterogeneity, margin, growth pattern, degree of enhancement, and peritumoral edema and apparent diffusion coefficient (ADC) values might provide supplementary information and contribute to the prediction of IDH genotypes as well [7, 10–13].

Our purpose was to investigate the predictive value of standard MR imaging features and ADC parameters in IDH mutation status of LGGs, so as to provide reliable imaging reference for molecular subtype prediction and prognosis evaluation.

Materials and methods

Patient selection

The Institutional Review Board of Xuanwu Hospital Capital Medical University approved this retrospective study, and informed consent was waved. Inclusion criteria were as follows: patients with newly diagnosed primary glioma performed MRI examinations including T2WI, FLAIR, DWI, pre- and post-enhanced T1WI simultaneously before treatment from 2013 to 2018; explicit pathological diagnosis of LGG according to the WHO classification system; available IDH mutation status. There were 74 evaluable patients included in the final cohort.

MRI acquisition protocol

All MR images were obtained on a 3-T unit (Verio, Siemens; Trio, Siemens) using an 8-channel head coil. The glioma imaging protocol included the following sequences: T1-weighted imaging (T1WI, TR/TE, 160 ms/3.05 ms; FOV, 240 mm × 240 mm; section thickness, 5 mm; matrix, 512 × 512), T2WI (TR/TE, 3800 ms/93 ms; FOV, 240 mm × 240 mm; section thickness, 5 mm; matrix, 512 × 512), FLAIR (TR/TE, 1800 ms/94 ms; FOV, 240 mm × 240 mm; section thickness, 5 mm; matrix, 128 × 128), and DWI (TR/TE, 5500 ms/90 ms; FOV, 240 mm × 240 mm; section thickness, 5 mm; matrix, 128 × 128, $b = 0$, 1000 s/mm^2). Contrast-enhanced T1WI (TR/TE, 160 ms/3.05 ms; FOV, 240 mm × 240 mm; section thickness, 5 mm; matrix, 512 × 512) were acquired after administering 0.1 mL/kg of gadopentetate dimeglumine.

Histopathologic analysis

The enrolled gliomas were classified into grade II or III by hematoxylin and eosin (H&E) staining. The status of IDH1 mutation was detected by immunohistochemical assay, a fast and reliable method for evaluation of the IDH1 gene mutation status [14], at the most common codon R132H [15]. If it was negative, further genomic sequencing analysis was performed to identify IDH1 and IDH2 mutations. The pathology was determined by two neuropathologists separately. If there was any different diagnosis, the consensus was reached by negotiation. Subsequently, the patients were classified into IDH-mutated and IDH-wildtype groups.

Image evaluation

MR imaging features were analyzed by two neuroradiologists who were both blinded to the histopathologic diagnosis, IDH mutation classification, and clinical information of patients. The MR imaging features were analyzed as follows: (1) tumor location, including 4 groups: (a) only one of frontal, temporal, parietal, or occipital lobe was invaded; (b) insular lobe combined with one or more other lobes invaded; (c) multilobes with or without corpus callosum invaded; (d) thalamus or brain stem invaded; (2) T2-FLAIR mismatch sign: presence or absence of a complete/near complete hyperintense signal on T2WI and relative hypointense signal on FLAIR with a ring-shaped hyperintense signal at the edge of tumor; (3) signal heterogeneity: homogeneous (the signal of tumor was homogenous) or heterogeneous signal intensity (the lesion displayed a mixed intensity) on T2WI and FLAIR; (4) tumor margin: tumor with sharp or indistinct margin; (5) tumor growth pattern: tumor that involved one side hemisphere was defined as unilateral growth, while both sides of hemisphere involved across corpus callosum was defined bilateral growth; (6) degree of enhancement: no, mild (the portion of enhancing area was < 50% of the tumor) or moderate to obvious (the portion of enhancing area was ≥ 50% of the tumor) enhancement; (7) degree of peritumoral edema: absence, mild (the longest diameter of edema was < 50% of the longest diameter of the tumor), moderate to obvious (the longest diameter of edema was ≥ 50% of the longest diameter of the tumor); (8) normalized minimum and mean ADC (nADCmin and nADCmean) values: quantitative ADC analysis was performed using PMOD version 3.505 (PMOD Ltd.). The ADC maps and FLAIR images were co-registered using non-affine deformations and manually adjusted by referring to anatomic landmarks. Subsequently, a region of interest (ROI) was generated

using a 3D semi-automatic contouring segmentation method subsuming the entire region of FLAIR hyperintensity by two experienced neuroradiologists in consensus to acquire the mean and minimum ADC (ADCmin and ADCmean). The average ADC value was also calculated from the centrum semiovale on the contralateral side of the tumor by drawing three circular ROI (size 30–40 mm^2). The normalized ADC (nADCmin and nADCmean) was obtained by dividing the tumor ADC by the average ADC of the contralateral normal-appearing white matter.

Statistical analysis

Cohen's Kappa statistics was performed using an inter-rater agreement analysis by MedCalc Statistical Software version 18.2.1 (MedCalc Software bvba, Ostend, Belgium) to determine the consistency between the two neuroradiologists after evaluating images. Different κ values indicate different levels of agreement: $\kappa \leq 0.20$ represents poor agreement, 0.21–0.40 represents fair agreement, 0.41–0.60 represents moderate agreement, 0.61–0.80 represents good agreement, and 0.81–1.00 represents great agreement.

Statistical analysis was performed using SPSS version 21.0 (SPSS, Inc., Chicago, IL, USA). The Chi-square test (or Fisher's exact test if the number of one subgroup was < 5) was used to compare the differences of MR imaging features in different IDH genotypes after reaching agreement of discordant results. The Shapiro–Wilk test was used to determine whether the numeric data (normalized ADC parameters) for each group were normally distributed. According to the non-normally distributed variables, nADCmin and nADCmean were compared using the Mann–Whitney U test between different subgroups. The optimal cut-off value, sensitivity, specificity, and area under the curve (AUC) of the ADC parameters with significant differences were calculated via receiver-operating characteristic (ROC) curves. Statistical significance was defined as $P < 0.05$ for all tests. To further explore the predictive value of T2-FLAIR mismatch sign in IDH-mutated LGG, sensitivity, specificity, positive predictive value (PPV), and negative predictive value (NPV)

were calculated based on the final consensus. Among imaging features and ADC parameters, significant variables in differentiating IDH-mutated from IDH-wildtype LGGs were selected using binary logistic regression models. The diagnostic performance of all imaging features to predict the IDH mutation status was assessed by ROC curve analysis.

Results

There were 74 patients (41 males, 33 females) in the final cohort consisted of 33 grade II and 41 grade III gliomas. They were divided into IDH-mutated ($n = 44$) and IDH-wildtype ($n = 30$). The clinical characteristics of patients are presented in Table 1. The overall average age was 44.77 ± 13.03 years (range 15–73 years). There were no significant differences in age or gender between the two groups.

Inter-rater agreement for imaging features

After independent analysis, inter-rater agreement for T2-FLAIR mismatch sign by two neuroradiologists reached the great level with κ value of 0.824 (95% confidence interval (CI): 0.658–0.990). Inter-rater agreement for signal heterogeneity ($\kappa = 0.494$, 95% CI: 0.296–0.691), tumor margin ($\kappa = 0.495$, 95% CI: 0.282–0.709), and degree of peritumoral edema ($\kappa = 0.473$, 95% CI: 0.314–0.632) reached moderate level. Tumor growth pattern ($\kappa = 0.643$, 95% CI: 0.404–0.882) and degree of enhancement ($\kappa = 0.689$, 95% CI: 0.552–0.825) reached good level.

T2-FLAIR mismatch sign for predicting IDH-mutated LGGs

Both neuroradiologists thought that the T2-FLAIR mismatch sign was presented in 12 cases (Fig. 1) and absent in 58 cases (Fig. 2). Four cases reached different opinions. The total of LGGs that manifested T2-FLAIR mismatch sign increased to 15 after negotiation. There was significant difference in T2-FLAIR mismatch sign of different

Table 1 Characteristics and distribution of IDH mutation subtypes

	IDH-mutated	IDH-wildtype	Total	t/χ^2	P
Age at diagnosis				−0.741	0.461
Mean	43.84 ± 12.14	46.13 ± 14.33	44.77 ± 13.03		
Range	25–73	15–68	15–73		
Gender				0.088	0.767
Male	25	16	41		
Female	19	14	33		
WHO grade II	22	11	33	–	–
WHO grade III	22	19	41	–	–

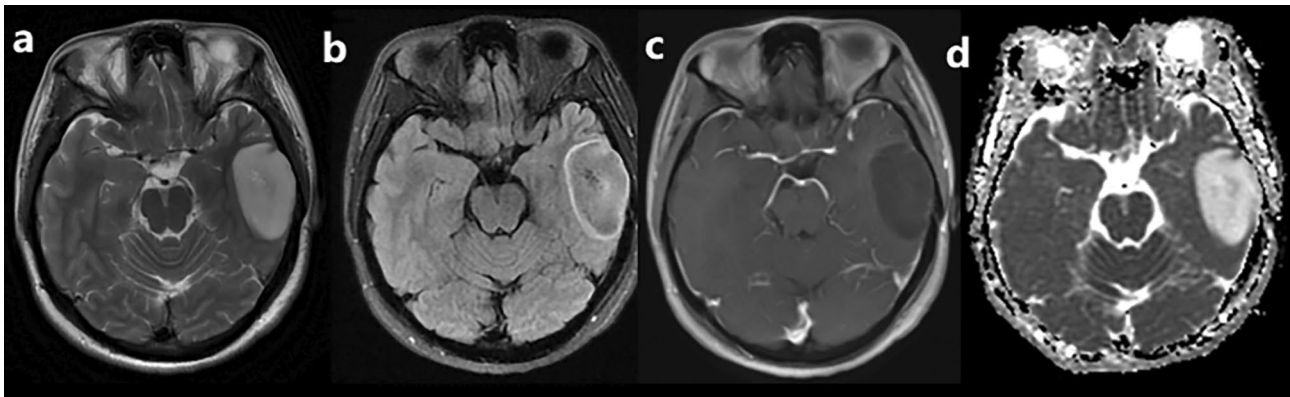*IDH* isocitrate dehydrogenase; *WHO* World Health Organization

Fig. 1 Example of IDH-mutated LGG with T2-FLAIR mismatch sign. A 31-year-old woman with a grade III IDH-mutated anaplastic astrocytoma in left temporal lobe. T2WI (**a**) shows almost complete hyperintense signal within the lesions, while FLAIR (**b**) shows relatively hypointense signal within the majority of the lesion, with a ring-shaped hyperintense signal at the edge of lesion. The lesion manifests distinct margin, almost no contrast enhancement (**c**), and without peritumoral edema. The ADC map (**d**) shows the tumor with an increased ADC value (nADCmean = 2.72, nADCmin = 2.60)
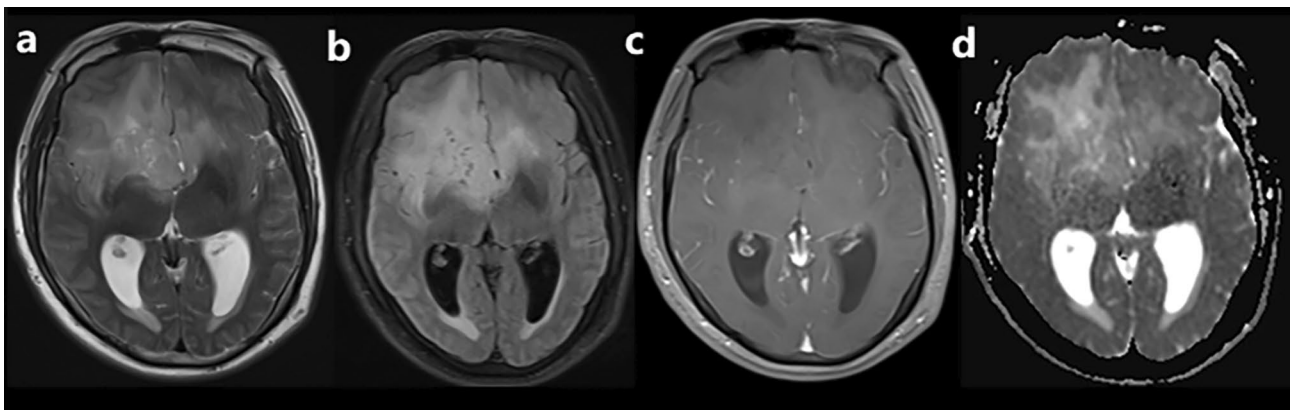

Fig. 2 Example of IDH-wildtype LGG without T2-FLAIR mismatch sign. A 45-year-old man with a grade III IDH-wildtype anaplastic astrocytoma in right frontal–temporal-insular lobe. **a–c** The lesion presents mild contrast enhancement and peritumoral edema with indistinct margin. The ADC map (**d**) shows the tumor with a lower ADC value than that of IDH-mutated LGGs (nADCmean = 1.41, nADCmin = 1.22)

IDH mutation genotypes ($P < 0.001$). Furthermore, all 15 cases that presented T2-FLAIR mismatch sign were IDH-mutated type, accounting for 34.09% of all IDH-mutated LGGs. T2-FLAIR mismatch sign was highly specific for IDH-mutated lower grade gliomas with the specificity and PPV of 100%, while the NPV and sensitivity were relative lower (50.85% and 34.09%, respectively).

Other MR imaging features for predicting IDH genotypes

After resolving the discordances of the two neuroradiologists about the imaging features, the comparisons of different imaging features in LGGs with different IDH mutation genotypes are summarized in Table 2. On conventional MRI, the signals of IDH-mutated and IDH-wildtype LGGs could be homogeneous or heterogeneous ($P = 0.938$). The margin of IDH-mutated LGGs was sharp and clear, while that of IDH-wildtype was undefined ($P = 0.003$). No significant difference was observed in the growth pattern between the two groups ($P = 0.160$). Most IDH-mutated LGGs showed less degree of internal enhancement ($P = 0.001$) and peritumoral edema ($P = 0.016$) than IDH-wildtype.

There was a significant difference in tumor location between the two genotypes ($P = 0.002$). IDH-mutated LGGs involved single lobe preferentially (83.87%), all of which was frontal or temporal lobe. By contrast, IDH-wildtype LGGs mainly manifested multiple lobes involvement, frequently with corpus callosum and insula invasion (55.56%,

Table 2 Comparison of imaging features in glioma with different IDH mutation status

MRI features	IDH-mutated, n (%)	IDH-wildtype, n (%)	κ	χ^2	P
T2-FLAIR mismatch			0.824	–	< 0.001
Positive	15/15 (100)	0/15 (0)			
Negative	29/59 (49.15)	30/59 (50.85)			
Location			–	13.303	0.002
Single lobe	26/31 (83.87)	5/31 (16.13)			
Insular	7/17 (41.18)	10/17 (58.82)			
Multilobes	9/19 (47.37)	10/19 (52.63)			
Thalamus or brain stem	2/7 (28.57)	5/7 (71.43)			
Signal heterogeneity			0.494	0.006	0.938
Homogeneous	18/30 (60.00)	12/30 (40.00)			
Heterogeneous	26/44 (59.09)	18/44 (40.91)			
Tumor margin			0.495	9.285	0.003
Distinct	20/24 (83.33)	4/24 (16.67)			
Indistinct	23/50 (46.00)	27/50 (54.00)			
Growth pattern			0.643	1.974	0.160
Unilateral	38/60 (63.33)	22/60 (36.67)			
Bilateral	6/14 (42.86)	8/14 (57.14)			
Contrast enhancement			0.689	–	0.001
Absent/mild	43/64 (67.19)	21/64 (32.81)			
Obvious	1/10 (10.00)	9/10 (90.00)			
Peritumoral edema			0.473	8.310	0.016
Absent	17/21 (80.95)	4/21 (19.05)			
Mild	22/38 (57.89)	16/38 (43.24)			
Obvious	5/15 (33.33)	10/15 (66.67)			

IDH isocitrate dehydrogenase

20/36). 71.4% (5/7) of gliomas invaded thalamus or brain-stem were IDH-wildtype.

The binary logistic regression analysis showed that there were significant differences in signal heterogeneity ($P = 0.030$), tumor margin ($P = 0.027$), and degree of enhancement ($P = 0.009$) of different IDH mutation genotypes. Three significant independent variables were screened: signal heterogeneity (X_1), tumor margin (X_2), and degree of enhancement (X_3). The regression equation was as follows: logit $(P) = 4.112 + 1.525X_1 - 1.994X_2 3.339X_3$ ($\chi^2 = 34.669$, $P < 0.001$). The ROC curve analysis showed that the sensitivity, specificity, and AUC of the model to predict IDH genotypes were 65.91%, 93.33%, and 0.892, respectively ($P < 0.001$, 95% CI: 0.798–0.952).

nADCmin and nADCmean values of IDH-mutant LGGs were significantly higher than those of IDH-wildtype (both $P < 0.001$) (Figs. 1d, 2d). The optimal cut-off values of nADCmin and nADCmean to differentiate IDH-mutated and IDH-wildtype LGGs were 1.234 and 1.503, respectively. The sensitivity, specificity, and AUC were 79.55% and 84.09%, 73.33% and 63.33%, and 0.817 and 0.808, respectively (both $P < 0.001$, Fig. 3). The ROC curve analysis showed that the sensitivity, specificity, and AUC of the combination of the imaging features and nADC parameters
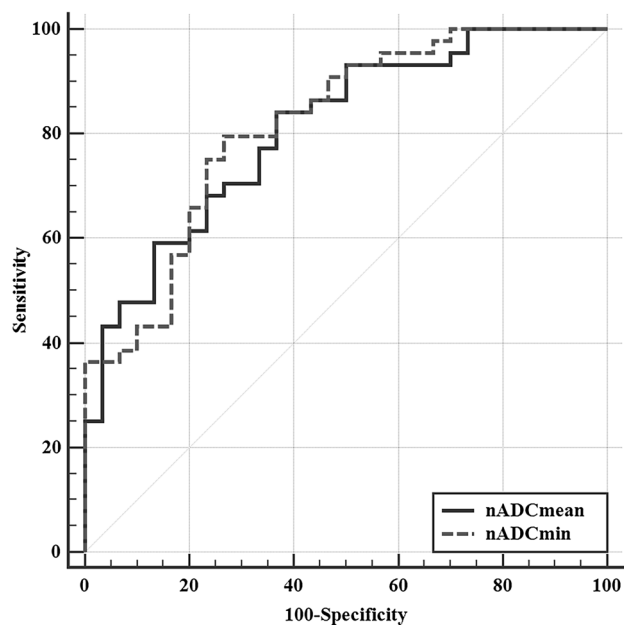

Fig. 3 Comparison of ROC curves of nADCmin and nADCmean in discriminating between IDH-mutated and IDH-wildtype LGGs

to predict IDH genotypes were 81.82%, 86.67%, and 0.925, respectively (*P* < 0.001, 95% CI:0.840–0.973).

Discussion

Our study demonstrated that the presence of T2-FLAIR mismatch sign as well as distinct margin, no or mild degree of enhancement and peritumoral edema, single-lobe involvement on standard MR images, and higher nADCmin and nADCmean values are helpful to distinguish IDH-mutated LGGs from IDH-wildtype preoperatively. Identifying above features on standard MRI is a convenient approach to predict IDH genotypes which requires no advanced examinations.

T2-FLAIR mismatch sign was first proposed by Patel et al. [9] and further validated by Broen et al. [16] among non-enhanced LGGs. Only recruiting non-enhanced LGGs may exclude a number of IDH-wildtype gliomas and result in a selection bias. In our study, we recruited LGGs with different degrees of enhancement to reduce the selection bias. As our result showed, patients who present T2-FLAIR mismatch sign were all IDH-mutated LGGs. Juratli et al. [17] identified 316 LGGs with different degree of contrast enhancement and found that gliomas with enhancement were more frequently seen in IDH-wildtype than in IDH-mutated genotype, which was consistent with the result of our study. They also found that T2-FLAIR mismatch sign was present in IDH-mutated gliomas including IDH-mutated astrocytomas and IDH-mutated with 1p/19q co-deleted oligodendrogliomas. Goyal et al. [18] found the specificity of T2-FLAIR mismatch sign in predicting the IDH or 1p/19q co-deletion status in diffuse LGGs were 100% and 54%, respectively. Kapsalaki et al. [19] evaluated the role of the T2-FLAIR mismatch sign in detecting IDH mutations of a mixed population with low- and high-grade gliomas. They found that T2-FLAIR mismatch sign co-registered with the degree of tumor homogeneity was significant predictors of the IDH status of gliomas, and the specificity of T2-FLAIR mismatch sign in the detection of the IDH-mutated gliomas was 86.7%. Several studies reported false -positive results for the T2-FLAIR mismatch sign, including dysembryoplastic neuroepithelial tumor, pediatric-type gliomas, and non-neoplastic lesions [20–22]. Jain et al. [23] summarized the imaging criteria for the T2-FLAIR mismatch sign to optimize its clinical use in glioma diagnostics. They pointed out that many of the reported false-positive cases were related to variable application of the sign's imaging criteria and differences in image acquisition, as well as to differences in the included patient populations.

However, the pathology of T2-FLAIR mismatch sign and why only part of the IDH-mutated LGGs manifested T2-FLAIR mismatch have been still ambiguous. There are some assumptions. First of all, some new molecular subtypes may exist among IDH-mutated LGGs which are still unknown to humans. It may be associated with the increasing of proteins in the mammalian target of rapamycin signaling pathway [23]. In addition, Tay et al. [26] found atypical imaging feature of protoplasmic astrocytoma (5/8) on MRI. It showed generally hyperintense on T2WI and manifested signal suppression in greater than 50% of lesions on FLAIR. The feature resembles to T2-FLAIR mismatch sign, but it has not been validated by molecular pathology. More microcyst changes in the central part of the lesions had been discovered by pathology than in the peritumoral high signal on FLAIR. Deguchi et al. [27] found that microcystic change was significantly associated with T2-FLAIR mismatch sign. T2-FLAIR mismatch sign may reflect microcyst formation in IDH-mutant astrocytomas.

In consideration of not all of the IDH-mutated LGGs present T2-FLAIR mismatch sign, we further observed the predictive value of other imaging features on standard MRI. After reaching a consensus about imaging features, we found tumor location, margin, degree of contrast enhancement, and peritumoral edema were different between IDH-mutated and wildtype gliomas. IDH-wildtype LGGs manifested stronger invasiveness on conventional MR images. It occurs at the junction of brain lobes frequently, such as corpus callosum, thalamus, and brainstem. It is more likely to involve insular lobe [28]. In contrast, IDH-mutated LGGs prefer to involve a single lobe, especially frontal or temporal lobe [10, 29]. IDH-mutated LGGs tend to manifest unilateral growth pattern with well-defined lesions, lower degree of enhancement, and peritumoral edema. The above findings were basically consistent with the previous studies [30, 31]. It is suggested that IDH-mutated LGGs may have a better prognosis than IDH-wildtype by affecting the location of tumors, such as frontal or temporal lobe that are easy to resect.

Furthermore, ADC calculated from DWI may supply quantitative information of tumor cellularity, which has been widely used in routine diagnosis of glioma. ADCmin could reflect the highest cellularity within the whole heterogeneous tumors. We demonstrated that both nADCmin and nADCmean of IDH-mutated LGGs were significantly higher than those of IDH-wildtype (AUC of 0.817 and 0.808, respectively), which is consistent with the results of previous studies [7, 32, 33]. Wu et al. [7] found that nADCmean could detect IDH mutation status with an optimal cut-off value of 1.2, sensitivity of 81.9%, specificity of 74.6%, and AUC of 0.790, regardless of the WHO grade. Xing et al. [34] found that the ADCmin and nADCmin of IDH-mutated lower grade astrocytomas were higher than those of IDH-wildtype. Furthermore, the sensitivity, specificity, and AUC of the combination of ADC parameters and other imaging features on standard MRI in the detection of IDH mutation status were 81.82%, 86.67%, and 0.925, respectively. These imaging features on standard MRI are easy to use and

helpful in recognizing IDH-mutated LGGs, particularly if formal IDH testing is not available.

There are some limitations in our study. First, the small sample size may influence the results, which need to be validated in a larger cohort. Second, we only detected IDH mutation status which is one of the most importance molecular of glioma. We failed to further analyze the relationships between the imaging features and other meaningful molecular biomarkers such as 1p/19q co-deletion because of the incomplete molecular pathological information. Third, only part of the patients underwent perfusion-weighted imaging or other advanced examinations. We will further investigate the value of advanced MR techniques in prediction of glioma genotypes. Finally, point-to-point biopsy in site of T2-FLAIR "match" and "mismatch" for molecular and pathophysiological analysis is recommended for future research.

Conclusion

The presence of T2-FLAIR mismatch sign, sharp tumor margin, less degree of contrast enhancement and peritumoral edema, and higher normalized ADC are more frequently found in IDH-mutated LGGs than in IDH-wildtype. This image-based approach incorporating imaging features on MR with ADC parameters of DWI could be easily applied in clinical practice and helpful for predicting IDH mutation status of LGGs non-invasively, and formulating individualized treatment decision.

Data availability All data are transparent.

Code availability Not applicable.

Declarations

Conflict of interest The authors declare no potential conflicts of interest.

Ethics approval The Institutional Review Board of Xuanwu Hospital Capital Medical University approved this retrospective study.

Informed consent The Institutional Review Board of Xuanwu Hospital Capital Medical University approved this informed consent was waved.

Consent for publication All authors agree to publish the article.

References

1. Chen WQ, Zheng RS, Baade PD, et al. Cancer statistics in China, 2015. Ca-cancer J Clin. 2016;66:115–32.
2. Rogers TW, Toor G, Drummond K, et al. The 2016 revision of the WHO classification of central nervous system tumours: retrospective application to a cohort of diffuse gliomas. J Neuro-oncol. 2018;137:181–9.
3. Jansen M, Yip S, Louis DN. Molecular pathology in adult gliomas: diagnostic, prognostic, and predictive markers. Lancet Neurol. 2010;9:717–26.
4. Cairncross JG, Wang MH, Jenkins RB, et al. Benefit from procarbazine, lomustine, and vincristine in oligodendroglial tumors is associated with mutation of IDH. J Clin Oncol. 2014;32:783.
5. Louis DN, Perry A, Reifenberger G, et al. The 2016 world health organization classification of tumors of the central nervous system: a summary. Acta Neuropathol. 2016;131:803–20.
6. Sabha N, Knobbe CB, Maganti M, et al. Analysis of IDH mutation, 1p/19q deletion, and PTEN loss delineates prognosis in clinical low-grade diffuse gliomas. Neuro Oncol. 2014;16:914–23.
7. Wu CC, Jain R, Radmanesh A, et al. Predicting genotype and survival in glioma using standard clinical MR imaging apparent diffusion coefficient images: a pilot study from The Cancer Genome Atlas. Am J Neuroradiol. 2018;39:1814–20.
8. Zhao B, Zhang C, Zhao X, et al. Stratification of grade of spinal cord non-ependymal gliomas by magnetic resonance imaging. World Neurosurg. 2019;125:e902–8.
9. Patel SH, Poisson LM, Brat DJ, et al. T2–FLAIR mismatch, an imaging biomarker for IDH and 1p/19q status in lower grade gliomas: a TCGA/TCIA project. Clin Cancer Res. 2017;23:6078–85.
10. Delfanti RL, Piccioni DE, Handwerker J, et al. Imaging correlates for the 2016 update on WHO classification of grade II/III gliomas: implications for IDH, 1p/19q and ATRX status. J Neuro-oncol. 2017;135:601–9.
11. Smits M, van den Bent MJ. Imaging correlates of adult glioma genotypes. Radiology. 2017;284:316–31.
12. Chen IE, Swinburne N, Tsankova NM, et al. Sequential apparent diffusion coefficient for assessment of tumor progression in patients with low-grade glioma. Am J Neuroradiol. 2018;39:1039–46.
13. Park YW, Han K, Ahn SS, et al. Prediction of IDH1-mutation and 1p/19q-codeletion status using preoperative MR imaging phenotypes in lower grade gliomas. Am J Neuroradiol. 2018;39:37–42.
14. Preusser M, Wohrer A, Stary S, Hoftberger R, Streubel B, Hainfellner JA. Value and limitations of immunohistochemistry and gene sequencing for detection of the IDH1-R132H mutation in diffuse glioma biopsy specimens. J Neuropath Exp Neur. 2011;70:715–23.
15. Lewandowska M, Furtak J, Szylberg T, et al. An analysis of the prognostic value of IDH1 (isocitrate dehydrogenase 1) mutation in polish glioma patients. Mol Diagn Ther. 2014;18:45–53.
16. Broen MPG, Smits M, Wijnenga MMJ, et al. The T2-FLAIR mismatch sign as an imaging marker for non-enhancing IDH-mutant, 1p/19q-intact lower grade glioma: a validation study. Neuro Oncol. 2018;20:1393–9.
17. Juratli TA, Tummala SS, Riedl A, et al. Radiographic assessment of contrast enhancement and T2/FLAIR mismatch sign in lower grade gliomas: correlation with molecular groups. J Neurooncol. 2019;141:327–35.
18. Goyal A, Yolcu YU, Goyal A, et al. The T2-FLAIR-mismatch sign as an imaging biomarker for IDH and 1p/19q status in diffuse

low-grade gliomas: a systematic review with a Bayesian approach to evaluation of diagnostic test performance. Neurosurg Focus. 2019;47:E13.

19. Kapsalaki EZ, Brotis AG, Tsikrika A, et al. The role of the T2-FLAIR mismatch sign as an imaging marker of IDH status in a mixed population of low- and high-grade gliomas. Brain Sci. 2020;10:874.

20. Onishi S, Amatya VJ, Kolakshyapati M, et al. T2-flair mismatch sign in dysembryoplasticneuroepithelial tumor. Eur J Radiol. 2020;126:108924.

21. Johnson DR, Kaufmann TJ, Patel SH, et al. There is an exception to every rule-T2-FLAIR mismatch sign in gliomas. Neuroradiology. 2019;61:225–7.

22. Lee MK, Park JE, Jo Y, et al. Advanced imaging parameters improve the prediction of diffuse lower grade gliomas subtype, IDH mutant with no 1p19q codeletion: added value to the T2/FLAIR mismatch sign. Eur Radiol. 2020;30:844–54.

23. Jain R, Johnson DR, Patel SH, et al. "Real world" use of a highly reliable imaging sign: "T2-FLAIR mismatch" for identification of IDH mutant astrocytomas. Neuro Oncol. 2020;22:936–43.

24. Xia P, Xu XY. PI3K/Akt/mTOR signaling pathway in cancer stem cells: from basic research to clinical application. Am J Cancer Res. 2015;5:1602–9.

25. Bai H, Harmanci AS, Erson-Omay EZ, et al. Integrated genomic characterization of IDH1-mutant glioma malignant progression. Nat Genet. 2016;48:59.

26. Tay KL, Tsui A, Phal PM, Drummond KJ, Tress BM. MR imaging characteristics of protoplasmic astrocytomas. Neuroradiology. 2011;53:405–11.

27. Deguchi S, Oishi T, Mitsuya K, et al. Clinicopathological analysis of T20FLAIR mismatch sign in lower grade gliomas. Sci Rep. 2020;10:10113.

28. Xiong J, Tan WL, Wen JB, et al. Combination of diffusion tensor imaging and conventional MRI correlates with isocitrate dehydrogenase 1/2 mutations but not 1p/19q genotyping in oligodendroglial tumours. Eur Radiol. 2016;26:1705–15.

29. Sonoda Y, Shibahara I, Kawaguchi T, et al. Association between molecular alterations and tumor location and MRI characteristics in anaplastic gliomas. Brain Tumor Pathol. 2015;32:99–104.

30. Metellus P, Coulibaly B, Colin C, et al. Absence of IDH mutation identifies a novel radiologic and molecular subtype of WHO grade II gliomas with dismal prognosis. Acta Neuropathol. 2010;120:719–29.

31. Bahrami N, Hartman SJ, Chang YH, et al. Molecular classification of patients with grade II/III glioma using quantitative MRI characteristics. J Neuro-oncol. 2018;139:633–42.

32. Thust SC, Hassanein S, Bisdas S, et al. Apparent diffusion coefficient for molecular subtyping of non-gadolinium-enhancing WHO grade II/III glioma: volumetric segmentation versus two-dimensional region of interest analysis. Eur Radiol. 2018;28:3779–88.

33. Xing Z, Yang X, She D, Lin Y, Zhang Y, Cao D. Noninvasive assessment of IDH mutational status in world health organization grade II and III astrocytomas using DWI and DSC-PWI combined with conventional MR imaging. Am J Neuroradiol. 2017;38:1138–44.

34. Tan W, Xiong J, Huang W, Wu J, Zhan S, Geng D. Noninvasively detecting isocitrate dehydrogenase 1 gene status in astrocytoma by dynamic susceptibility contrast MRI. J Magn Reson Imagin. 2017;45:492–9.